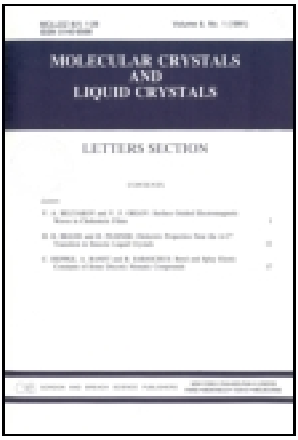

Molecular Crystals and Liquid Crystals
Publication details, including instructions for authors and subscription information:
http://www.tandfonline.com/loi/gmcl20

Sensitivity Analysis of Edge Sealing Process Parameters of Vacuum Glazing Panel

Youngshin Kim [a] & Euysik Jeon [a]

[a] Department of Mechanical Engineering , Kongju National University , Chungcheongnam-do , 331-717 , Korea

Published online: 08 Jan 2014.

To cite this article: Youngshin Kim & Euysik Jeon (2013) Sensitivity Analysis of Edge Sealing Process Parameters of Vacuum Glazing Panel, Molecular Crystals and Liquid Crystals, 585:1, 15-24, DOI: 10.1080/15421406.2013.852770

To link to this article: http://dx.doi.org/10.1080/15421406.2013.852770

Mol. Cryst. Liq. Cryst., Vol. 585: pp. 15–24, 2013

ISSN: 1542-1406 print/1563-5287 online
DOI: 10.1080/15421406.2013.852770

Sensitivity Analysis of Edge Sealing Process Parameters of Vacuum Glazing Panel

YOUNGSHIN KIM AND EUYSIK JEON*

Department of Mechanical Engineering, Kongju National University, Chungcheongnam-do 331-717, Korea

The edge sealing process of vacuum glazing panel manufacture is one that requires high reliability in order to maintain a vacuum state between two sheets of glass. In this study, a method of melting and sealing two sheets of glass using the hydrogen mixed gas torch during edge sealing was conducted. During melting and sealing, the deflection effect of the edge part is affected by process parameters such as flow rate of hydrogen mixed gas, moving speed of torch, and distance between the torch and the glass, among others. In order to analyze the correlative relationship of the shape prediction and the sealing shape of the edge part according to the process parameters, data was obtained by conducting sealing experiments and setting shape parameters for the lower melting part. A mathematical experiment equation that can predict the shape of the lower edge part according to the process parameters was developed by conducting nonlinear multiple regression analysis based on the data obtained for the shape parameters. In addition, sensitivity analysis according to the changes in the process parameters was carried out and the effects of the process parameters on the edge shape parameters were analyzed by using the developed mathematical equation.

Keywords Edge sealing; nonlinear multiple regression analysis; process parameters; Sensitivity analysis; vacuum glazing panel

Introduction

As a manufacturing process of display devices, glass edge sealing is a very important technique that requires a high level of reliability in order to maintain the vacuum condition. This process has in the past been conducted by using lasers and frit, among other devices [1,2]. Especially, glass sealing using frit has been widely applied in the fields of Plasma Display Panels (PDP) and LCDs, and in many other fields as well [3–5]. The extended application of edge sealing technology using frit, which maintains the high vacuum state, makes it feasible for use in many fields including not only display units but also home electronic appliances and windows and doors that require heat insulation. However, a problem of strength degradation is generated in cases in which the frit is exposed to the outside. There is demand for using frit without lead components due to recent reinforced regulations on using environment contaminating substances [6,7]. In this study, in order to expand and apply the process of edge sealing using frit into the PDP manufacturing

*Address correspondence to Prof. Euysik Jeon, Department of Mechanical Engineering, Kongju National University College of Engineering, Budae-dong, Seobuk-gu, Cheonan-si, Chungcheongnam-do 331-717, Korea. Tel.: (+82)41-521-9296; Fax: (+82)505-115-9284. E-mail: osjun@kongju.ac.kr

process and to dozens of fields of potential application, a technique was used in which we use hydrogen mixed gas to melt the edge part in order to seal two sheets of glass. In this process, the shape of the edge part is much affected by the process parameters; the flow rate of the hydrogen mixed gas, the moving speed of the torch. And the distance between the torch and the glass strongly affect the changes in edge shape and were selected as the three process parameters. In order to express the shape of the edge part, a total of 10 shape parameters were selected for the lower edge part. Edge sealing tests were conducted based on the selected parameters; data on the shape parameters were obtained by cutting the sealed sides. Based on these data, nonlinear multiple regression analysis was conducted to develop a mathematical experiment equation that can predict shapes according to the process parameters. In addition, the derived mathematical equation was differentiated according to each process parameter in order to verify the influence of the process parameters for the sensitivity analysis of the cross-sectional shape according to changes in the process parameters.

Edge Sealing Experiment

After placing a feeler gauge to maintain the gap between two sheets of soda-lime glass with dimensions of 160 mm$\times$100 mm$\times$3 mm, sample was placed in a furnace. Figure 1 shows the composition of the edge sealing system. We used a composite furnace in order to prevent the breaking and deformation of the glass due to thermal shock during edge sealing; we used a control panel to control the temperature of the furnace and the hydrogen mixed gas torch; a torch transfer system was used to control the moving speed of the torch, and coolant was used to control the cooling of the torch and the gas generator.

Selection of Process Parameters

During melting and sealing of the glass edge, the edge shape is affected by many process parameters. Among the many process parameters such as angle of torch, distance between the torch and the glass, moving speed of the torch, gas flow rate, and others, three parameters (gas flow rate (Q), moving speed of torch (V), and distance between the torch and the glass

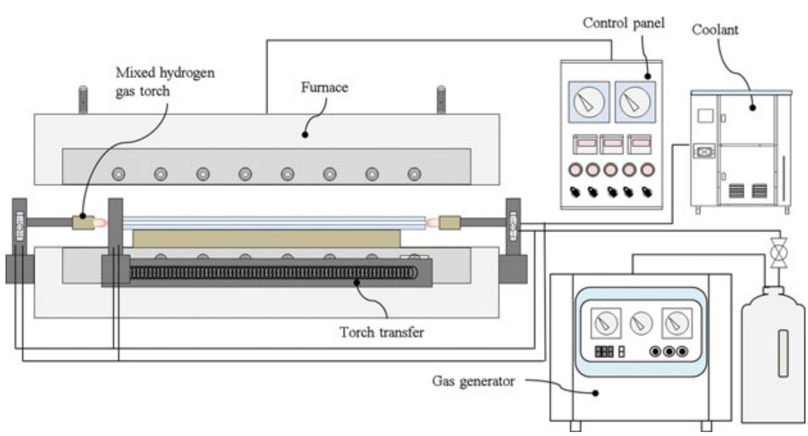

Figure 1. Composition of experiment apparatus.

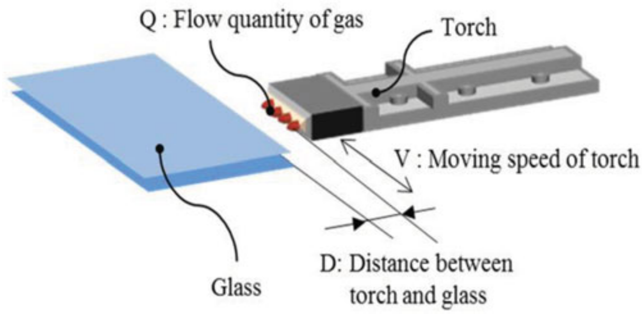

Figure 2. Conceptual scheme of process parameters.

(D)) that are considered to have greatest effect on the edge process parameter shape were selected as the process parameters. Figure 2 shows a conceptual scheme of the process parameters.

Selection of Edge Shape Parameters

Figure 3 is a cross-sectional photo of the glass sealed through the basic experiment. Figure 4 shows a conceptual scheme of the edge sealing shape, based on Fig. 3. As can be seen in these figures, the cross-section of the melting/sealing part appears in various shapes. While the shape of the upper glass edge sealing part has high reproducibility, the lower part shows various shapes depending on changes in the process parameters; in addition, partial deflection can also be observed. For the shape parameters of the cross-section, distances (L0∼L9) between the origin (O) and each of 10 points on the lower sealing cross-section were selected as the shape parameters, as shown in Fig. 5, which illustrates well the characteristics of the cross-section.

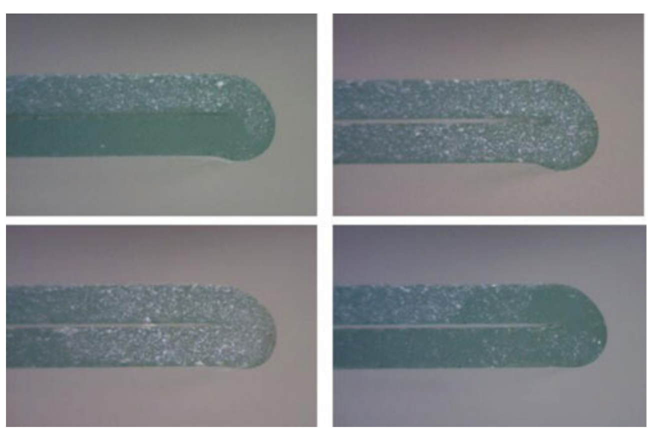

Figure 3. Cross-section of glass edge sealing.

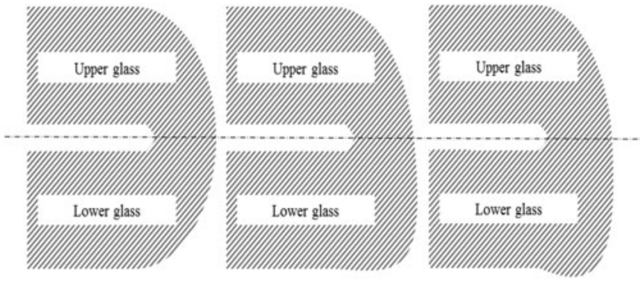

Figure 4. Conceptual scheme of cross-sectional shape.

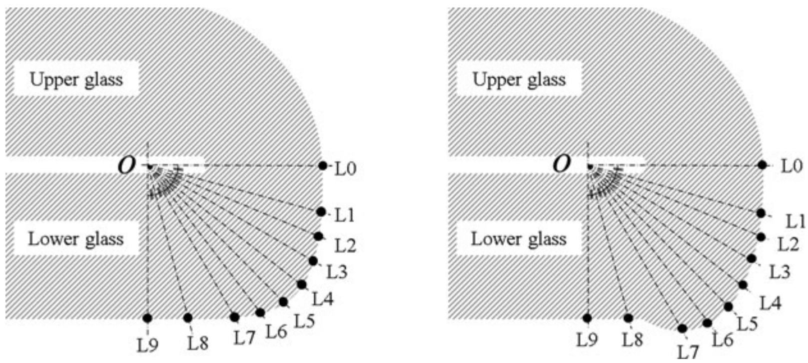

Figure 5. Selection of shape parameters.

Test Results

The process parameters were selected and the sealing experiment was conducted using the orthogonal array method of 3 factors and 3 levels. Data on the shape parameters from the sealing test results were obtained by image processing with Matlab; Table 1 shows the measurement results of the process conditions and shape parameters.

Table 1. Measurement results of process conditions and shape parameters

Q (#/min)	V (mm/sec)	D (mm)	L0	L1	L2	L3	L4	L5	L6	L7	L8	L9
10	3	3	4.7	4.9	4.9	4.9	4.8	4.6	4.3	3.8	2.9	2.9
10	4	4	5.0	5.1	5.0	4.9	4.6	4.0	3.6	3.2	2.9	2.9
11	3	4	4.6	4.9	5.0	4.9	4.8	4.6	4.3	3.8	3.1	2.9
11	4	5	4.7	4.9	4.9	4.7	4.5	4.1	3.7	3.3	2.9	2.9
11	5	3	5.1	5.2	5.2	5.0	4.7	4.1	3.7	3.4	3.1	2.9
12	3	5	4.5	4.7	4.8	4.9	4.9	4.7	4.6	4.3	3.5	3.1
12	4	3	5.0	5.4	5.4	5.3	5.0	4.6	4.0	3.4	2.9	2.9
12	5	4	5.2	5.2	5.2	5.0	4.7	4.4	3.9	3.4	3.1	2.9

The Derivations of Experiment Equation

A mathematical experiment equation was developed as shown in Equation (1) by conducting nonlinear regression analysis. For the developed test equations, equations were derived for each of the shape parameters; these equations are given as Equations (2)∼(11).

$$f_{Li}(Q, V, D) = a_{Li}\, Q^{b_{Li}}\, V^{c_{Li}}\, D^{d_{Li}} \begin{cases} \text{Q} & : \text{Gas flow rate} \\ \text{V} & : \text{Moving speed of torch} \\ \text{D} & : \text{Distance between torch and glass} \\ a_{Li}\sim d_{Li} & : \text{Coefficients} \end{cases} \tag{1}$$

$$f_{L0}(Q, V, D) = 10^{0.6212} \times \text{Q}^{-0.0232} \times \text{V}^{0.2162} \times \text{D}^{-0.0627} \tag{2}$$

$$f_{L1}(Q, V, D) = 10^{0.5585} \times \text{Q}^{0.1159} \times \text{V}^{0.1363} \times \text{D}^{-0.0989} \tag{3}$$

$$f_{L2}(Q, V, D) = 10^{0.5285} \times \text{Q}^{0.1880} \times \text{V}^{0.0733} \times \text{D}^{-0.1127} \tag{4}$$

$$f_{L3}(Q, V, D) = 10^{0.5093} \times \text{Q}^{0.2398} \times \text{V}^{-0.0015} \times \text{D}^{-0.1134} \tag{5}$$

$$f_{L3}(Q, V, D) = 10^{0.4492} \times \text{Q}^{0.3443} \times \text{V}^{-0.1149} \times \text{D}^{-0.1167} \tag{6}$$

$$f_{L4}(Q, V, D) = 100.2587 \times \text{Q}^{0.5899} \times \text{V}^{-0.2753} \times \text{D}^{-0.1264} \tag{7}$$

$$f_{L6}(Q, V, D) = 10^{0.2549} \times \text{Q}^{0.6019} \times \text{V}^{-0.3957} \times \text{D}^{-0.0960} \tag{8}$$

$$f_{L7}(Q, V, D) = 10^{0.3131} \times \text{Q}^{0.4611} \times \text{V}^{-0.4059} \times \text{D}^{-0.0169} \tag{9}$$

$$f_{L8}(Q, V, D) = 10^{0.0428} \times \text{Q}^{0.4418} \times \text{V}^{-0.1128} \times \text{D}^{0.0802} \tag{10}$$

$$f_{L9}(Q, V, D) = 10^{0.2876} \times \text{Q}^{0.1724} \times \text{V}^{-0.0292} \times \text{D}^{0.0255} \tag{11}$$

Prediction of the cross-sectional shape according to each process parameter is made possible by using the developed mathematical equation; the validity of the mathematical equation was confirmed by conducting ANOVA analysis. Table 2 shows the standard error of the estimate, the coefficient of multiple correlation, and the coefficient of determination of the mathematical equation.

Table 2. ANOVA of the mathematical models

No. of equation	Standard error of estimate	Coefficient of multiple correlation	Coefficient of determination (%)
2	0.0099	0.9467	89.63
3	0.0104	0.9149	83.71
4	0.0074	0.9342	87.29
5	0.0079	0.8894	79.10
6	0.0056	0.9589	91.96
7	0.0093	0.9673	93.57
8	0.0185	0.9322	86.90
9	0.0278	0.8704	75.77
10	0.0241	0.7359	54.17
11	0.0067	0.8045	64.77

Sensitivity Analysis

In order to analyze the effects of process parameters on shape changes, sensitivity analysis was conducted by differentiating the developed mathematical equation according to each of the process parameters. In order to analyze the sensitivity of the cross-sectional shape according to changes in the gas flow rate (Q), the derived equations (2∼11) were each differentiated by gas flow rate (Q). Equations (12)∼(21) show the sensitivity of the cross-sectional shape (L0∼L9) according to changes in the gas flow rate (Q). Moreover, for sensitivity analysis of the cross-sectional shape according to changes in the moving speed of the torch (V) and the distance between the torch and the glass (D), the mathematical equation was differentiated according to each of the process parameters. Equations 22∼31 show the sensitivity according to changes in the moving speed of the torch (V), equations 32∼41 show the sensitivity according to the distance between the torch and the glass (D).

$$\frac{\partial f_{L0}(Q, V, D)}{\partial Q} = -0.0970 \times \mathrm{Q}^{-1.0232} \times \mathrm{V}^{0.2162} \times \mathrm{D}^{-0.0627} \tag{12}$$

$$\frac{\partial f_{L1}(Q, V, D)}{\partial Q} = 0.4194 \times \mathrm{Q}^{-0.8841} \times \mathrm{V}^{0.1363} \times \mathrm{D}^{-0.0989} \tag{13}$$

$$\frac{\partial f_{L2}(Q, V, D)}{\partial Q} = 0.6348 \times \mathrm{Q}^{-0.8120} \times \mathrm{V}^{0.0733} \times \mathrm{D}^{-0.1127} \tag{14}$$

$$\frac{\partial f_{L3}(Q, V, D)}{\partial Q} = 0.7747 \times \mathrm{Q}^{-0.7602} \times \mathrm{V}^{-0.0015} \times \mathrm{D}^{-0.1134} \tag{15}$$

$$\frac{\partial f_{L4}(Q, V, D)}{\partial Q} = 0.9686 \times \mathrm{Q}^{-0.6557} \times \mathrm{V}^{-0.1149} \times \mathrm{D}^{-0.1167} \tag{16}$$

$$\frac{\partial f_{L5}(Q, V, D)}{\partial Q} = 1.0702 \times \mathrm{Q}^{-0.4101} \times \mathrm{V}^{-0.2753} \times \mathrm{D}^{-0.1264} \tag{17}$$

$$\frac{\partial f_{L6}(Q, V, D)}{\partial Q} = 1.0825 \times \mathrm{Q}^{-0.3981} \times \mathrm{V}^{-0.3957} \times \mathrm{D}^{-0.0960} \tag{18}$$

$$\frac{\partial f_{L7}(Q, V, D)}{\partial Q} = 0.9482 \times \mathrm{Q}^{-0.5389} \times \mathrm{V}^{-0.4059} \times \mathrm{D}^{-0.0169} \tag{19}$$

$$\frac{\partial f_{L8}(Q, V, D)}{\partial Q} = 0.4876 \times \mathrm{Q}^{-0.5582} \times \mathrm{V}^{-0.1128} \times \mathrm{D}^{0.0802} \tag{20}$$

$$\frac{\partial f_{L9}(Q, V, D)}{\partial Q} = 0.3343 \times \mathrm{Q}^{-0.8276} \times \mathrm{V}^{-0.0292} \times \mathrm{D}^{0.0255} \tag{21}$$

$$\frac{\partial f_{L0}(Q, V, D)}{\partial V} = 0.9038 \times \mathrm{Q}^{-0.0232} \times \mathrm{V}^{-0.7838} \times \mathrm{D}^{-0.0627} \tag{22}$$

$$\frac{\partial f_{L1}(Q, V, D)}{\partial V} = 0.4932 \times \mathrm{Q}^{0.1159} \times \mathrm{V}^{-0.8637} \times \mathrm{D}^{-0.0989} \tag{23}$$

$$\frac{\partial f_{L2}(Q, V, D)}{\partial V} = 0.2475 \times \mathrm{Q}^{0.1880} \times \mathrm{V}^{-0.9267} \times \mathrm{D}^{-0.1127} \tag{24}$$

$$\frac{\partial f_{L3}(Q, V, D)}{\partial V} = -0.0048 \times \mathrm{Q}^{0.2398} \times \mathrm{V}^{-1.0015} \times \mathrm{D}^{-0.1134} \tag{25}$$

$$\frac{\partial f_{L4}(Q,V,D)}{\partial V} = -0.3232 \times Q^{0.3443} \times V^{-1.1149} \times D^{-0.1167} \quad (26)$$

$$\frac{\partial f_{L5}(Q,V,D)}{\partial V} = -0.4995 \times Q^{0.5899} \times V^{-1.2753} \times D^{-0.1264} \quad (27)$$

$$\frac{\partial f_{L6}(Q,V,D)}{\partial V} = -0.7116 \times Q^{0.6019} \times V^{-1.3957} \times D^{-0.0960} \quad (28)$$

$$\frac{\partial f_{L7}(Q,V,D)}{\partial V} = -0.8347 \times Q^{0.4611} \times V^{-1.4059} \times D^{-0.0169} \quad (29)$$

$$\frac{\partial f_{L8}(Q,V,D)}{\partial V} = -0.1245 \times Q^{0.4418} \times V^{-1.1128} \times D^{0.0802} \quad (30)$$

$$\frac{\partial f_{L9}(Q,V,D)}{\partial V} = -0.0566 \times Q^{0.1724} \times V^{-1.0292} \times D^{0.0255} \quad (31)$$

$$\frac{\partial f_{L0}(Q,V,D)}{\partial D} = -0.2621 \times Q^{-0.0232} \times V^{0.2162} \times D^{-1.0627} \quad (32)$$

$$\frac{\partial f_{L1}(Q,V,D)}{\partial D} = -0.3578 \times Q^{0.1159} \times V^{0.1363} \times D^{-1.0989} \quad (33)$$

$$\frac{\partial f_{L2}(Q,V,D)}{\partial D} = -0.3806 \times Q^{0.1880} \times V^{0.0733} \times D^{-1.1127} \quad (34)$$

$$\frac{\partial f_{L3}(Q,V,D)}{\partial D} = -0.3664 \times Q^{0.2398} \times V^{-0.0015} \times D^{-1.1134} \quad (35)$$

$$\frac{\partial f_{L4}(Q,V,D)}{\partial D} = -0.3283 \times Q^{0.3443} \times V^{-0.1149} \times D^{-1.1167} \quad (36)$$

$$\frac{\partial f_{L5}(Q,V,D)}{\partial D} = -0.2293 \times Q^{0.5899} \times V^{-0.2753} \times D^{-1.1264} \quad (37)$$

$$\frac{\partial f_{L6}(Q,V,D)}{\partial D} = -0.1727 \times Q^{0.6019} \times V^{-0.3957} \times D^{-1.0960} \quad (38)$$

$$\frac{\partial f_{L7}(Q,V,D)}{\partial D} = -0.0348 \times Q^{0.4611} \times V^{-0.4059} \times D^{-0.9186} \quad (39)$$

$$\frac{\partial f_{L8}(Q,V,D)}{\partial D} = 0.0885 \times Q^{0.4418} \times V^{-0.1128} \times D^{-0.9745} \quad (40)$$

$$\frac{\partial f_{L9}(Q,V,D)}{\partial D} = 0.0494 \times Q^{0.1724} \times V^{-0.0292} \times D^{0.0255} \quad (41)$$

Discussion of Results

The sensitivity for L0∼L9 was confirmed by applying the gas flow rate (Q : 10∼12(ℓ/min)), edge sealing speed (V : 3∼5(mm/sec)), and distance between the torch and the glass (D : 3∼5(mm)) to the derived sensitivity equations (12∼41). Figures 6–8 show in bar graph form the sensitivity of the shape parameters according to changes in each of the process parameters.

Figure 6 shows the sensitivity of the shape parameters L0∼L9 according to changes in the gas flow rate (Q). Although L0 shows a lower sensitivity compared to those of L1∼L9, it shows characteristics of being inversely proportional to the gas flow rate (Q). L4∼L7,

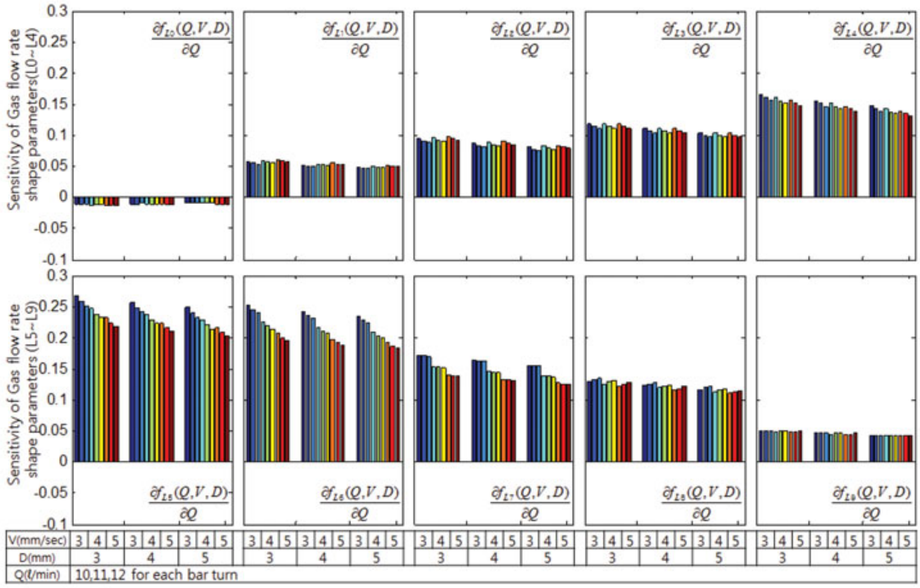

Figure 6. Sensitivity analysis of shape parameters according to changes in gas flow rate.

which can appear to be deflections of the cross-sectional shape, show high sensitivity to changes in the gas flow rate (Q). They especially showed higher sensitivity values for the gas flow rate (Q) as the distance between the torch (D) and the glass became lower and the moving speed of the torch (V) became faster.

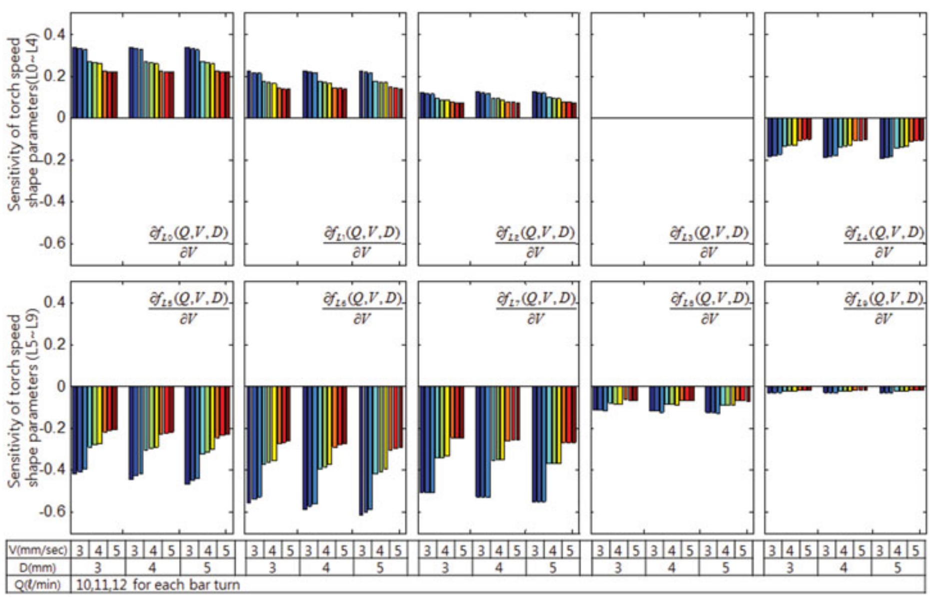

Figure 7. Sensitivity analysis of shape parameters according to changes in moving speed of torch.

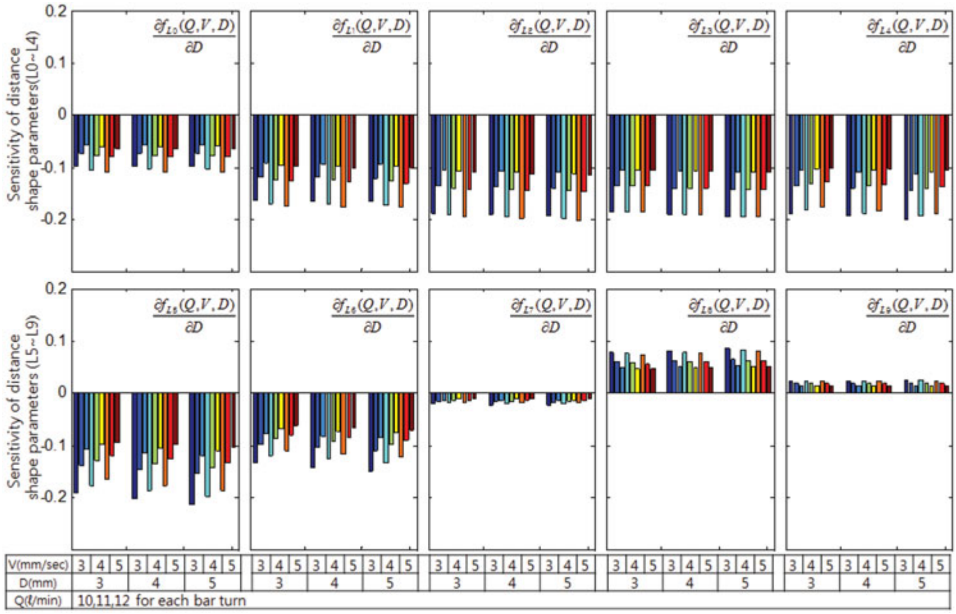

Figure 8. Sensitivity analysis of shape parameters according to changes in distance between torch and glass.

Figure 7 shows the sensitivity of the shape parameters (L0∼L9) according to changes in the moving speed of the torch (V). L4 had the lowest sensitivity to the moving speed of the torch (V); with this parameter as the basis for the before and after tests, L0∼L3 are found to be proportional to the moving speed of the torch (V), whereas L5∼L9 are inversely proportional. Furthermore, shape parameters L1 and L5∼L7 show high sensitivity to changes in moving speed of the torch (V); this sensitivity especially increases as the distance between the torch and the glass becomes lower. However, changes in the sensitivity according to changes in the gas flow rate (Q) are not that noticeable.

Figure 8 shows the sensitivity of the shape of the edge sealing part according to changes in the distance between the torch and the glass (D). Having L7 as the basis for the before and after tests, the sensitivity of the shape parameter according to the distance between the torch and the glass (D) changes from a negative to a positive number. This signifies that as the distance between the torch and the glass (D) increases, test result values of L0∼L6 decrease, whereas the test results of L8 and L9 increase. In addition, L0∼L6 show higher sensitivity to changes in the distance between the torch and the glass (D) than do samples L7∼L9. Changes in the sensitivity according to the distance between the torch and the glass (D) are most closely related to changes in the flow rate (Q), among all of the process parameters.

Analysis of the sensitivity of L0, which can be expressed as the width of the sealing part, and that of L4∼L7, which can be expressed as the deflection effect among the shape parameters, shows that the shape parameter L0 showed the highest sensitivity in proportion to the moving speed of the torch (V); L0 also shows a sensitivity that is inversely proportional to the distance between the torch (D) and the glass and to the gas flow rate (Q). Furthermore, L4∼L7 showed the highest sensitivity to changes in the moving speed of the torch (V), as these values were inversely proportional; this was followed by gas flow rate (Q) and distance between torch and glass (D).

Conclusions

In this study, in order to predict the shape of a melting part during melting/sealing of the edge part of a vacuum glazing panel, process (Q, V, D) and shape (L0∼L9) parameters were selected and a mathematical model was developed for their relationship through non-linear multiple regression analysis. In addition, sensitivity analysis of the shape parameters according to changes in the process parameters was conducted. Shape characteristics such as deflection during edge melting/sealing take place at the lower edge part and show the greatest sensitivity to changes in the moving speed of the torch (V); this is followed by sensitivity to the flow rate of the gas (Q) and to the distance between the torch and the glass (D). Decreased deflection was observed as the moving speed of the torch increased; higher sensitivity to changes in the gas flow rate was observed as the distance between the torch and the glass decreased and speed dropped.

Acknowledgment

This research was financially supported by the Ministry of Education, Science Technology (MEST) and National Research Foundation of Korea (NRF) through the Human Resource Training Project for Regional Innovation and the research grant of the Kongju National University in 2011.

References

[1] Lee, D.-J., Lee, Y.-H., Jang, J., & Ju, B.-K. (2001). *Sens. Actuators, A.*, *89*, 43–48.
[2] Peili, C. X. Y., Jiajie, T., Gaowei, X., & Le, L. (2012). *Microelectron. Eng.*, *100*, 6–11.
[3] Andreola, F., Barbieri, L., Corradi, A., & Lancellotti, I. (2007). *J. Eur. Ceram. Soc.*, *27*, 1623–1629.
[4] Yang, L., Tu, Y., Zhang, X., Li, Q., Wu, Z., & Wang, B. (2010). *Thin Solid Films*, *518*, 6268–6276.
[5] Wild, M. J., Gillner, A., & Poprawe, R. (2001). *Sens. Actuators, A.*, *93*, 63–69.
[6] Seo, D. S., Park, S. H., & Lee, J. K. (2009). *Curr. Appl. Phys.*, *9*, 72–S74.
[7] Yi, J. H., Koo, H. Y., Kim, J. H., Ko, Y. N., Hong, Y. J., Kang, Y. C., & Lee, H. M. (2011). *J. Alloys Compd.*, *509*, 6325–6331.